Extensions to NIFO and CRP to Estimate Frequency-Independent Nonlinear Parameters

Michael Kwarta[1], Matthew S. Allen[2]

[1]Graduate Student, [2]Professor, UW–Madison, Department of Engineering Mechanics
email: [kwarta, matt.allen]@wisc.edu

Abstract

The Nonlinear Identification through Feedback of the Output (NIFO) and Conditioned Reverse Path (CRP) methods are a popular family of approaches for nonlinear system identification. They estimate the underlying linear Frequency Response Function (FRF) as well as the parameters describing the mechanical system's nonlinearities. However, one troubling aspect is that the parameters obtained are complex numbers and typically are found to vary with frequency, so post-processing must be employed to obtain physically reasonable parameters and an accurate estimate of the underlying FRFs. This work proposes two methods (based on the $\mathbf{H}_1$ and $\mathbf{H}_2$ algorithms) which can be used in the estimation of the linear FRF as well as frequency-independent nonlinear parameters. This paper evaluates the methods numerically using a single degree of freedom system and exploring various methods for determining which nonlinear parameters to include in the model.

Keywords: NIFO methods, NIXO methods, Nonlinear System Identification, Black-box methods, Nonlinear parameters estimation

Introduction

The Nonlinear Identification through Feedback of the Output (NIFO) method and Conditioned Reverse Path (CRP) are popular approaches for nonlinear system identification. They estimate the underlying linear Frequency Response Function (FRF) as well as the parameters describing the mechanical system's nonlinearities. The $\mathbf{H}_1$-based NIFO method was first proposed in [1], while its twin algorithm, based on the $\mathbf{H}_2$ estimator, in [2]. Both NIFO algorithms have been sucessfully used in the estimation of the linear frequency response together with the parameters describing system's nonlinearity. However, one troubling aspect is that the parameters obtained are complex numbers and typically are found to vary with frequency, so post-processing must be employed to obtain physically reasonable parameters [3, 4].

This work proposes two methods (based on the $\mathbf{H}_1$ and $\mathbf{H}_2$ algorithms) which can be used in the estimation of the linear FRF as well as frequency-independent nonlinear parameters. Since these two new methods allow for system identification via augmenting the number of outputs, we call them *NIXO methods* – for *Nonlinear Identification through eXtended Outputs*. The methods are first evaluated numerically using a single degree of freedom system. Moreover, a strategy for utilizing the NIXO approaches in the black-box identification of a single degree of freedom mechanical system is presented.

In a future work, both NIXO methods will be employed experimentally to identify the physical parameters describing the nonlinearity of a 3D printed beams for oscillations near their first resonance frequencies. The results will be then used to compute the NNM backbone curve and compared to the solution obtained by another estimation algorithm and data collected using the well-established testing approach.

Derivation of NIFO and NIXO methods

In this section, the theory behind the three different nonlinear system identification algorithms is presented. These three algorithms are:

- $\mathbf{H}_1$– and $\mathbf{H}_2$–based NIFO methods that were previously proposed by Adams et al. [1, 2] (also known as the modified $\mathbf{H}_1$ and $\mathbf{H}_2$ algorithms),
- Two new $\mathbf{H}_1$– and $\mathbf{H}_2$–based algorithms dubbed Nonlinear Identification through eXtended Outputs ($\mathbf{H}_1$-NIXO and $\mathbf{H}_2$-NIXO) and
- Two new $\mathbf{H}_1$– and $\mathbf{H}_2$–based algorithms dubbed Nonlinear Identification through eXtended Outputs with Linear Data Provided ($\mathbf{H}_1$-NIXO-LDP and $\mathbf{H}_2$-NIXO-LDP).

The derivations start with steps common for all the algorithms, then they fork and focus on each method separately. For simplicity, we consider a single degree of freedom (SDOF) mechanical system described with equations of motion (EOM) defined in Eqs. (1) or (2), yet we believe that the algorithms can be generalized to MDOF systems.

$$m\ddot{x} + c\dot{x} + kx + c_2\dot{x}|\dot{x}| + k_3x^3 = f(t), \tag{1}$$

$$m\ddot{x} + c\dot{x} + kx + c_2\dot{x}^2 + k_3x^3 = f(t), \tag{2}$$

where $m,\ c,\ k,\ c_2$ and k_3 are *real* and *constant* parameters, $x(t)$ is the response of the system excited for certain initial conditions with a forcing function $f(t)$. If the individual time functions are expressed as in (3), then Eqs. (1) or (2) become equivalent to Eq. (4) with $D(\Omega) = k - m\Omega^2 + ic\Omega$ and *frequency–independent* c_2 and k_3. Equation (4) is true for every individual frequency Ω, where $\Omega \in \{\Omega_1, 2\Omega_1, \ldots, n\Omega_1\}$, n is the number of frequency samples and Ω_1 is the lowest of the frequencies considered.

$$\begin{aligned}
x(t) &= \mathrm{Re}\Big\{\sum_{k=1}^{n} X^k\ e^{ik\Omega_1 t}\Big\} \qquad f(t) = \mathrm{Re}\Big\{\sum_{k=1}^{n} F^k\ e^{ik\Omega_1 t}\Big\} \\
\dot{x}(t)|\dot{x}(t)| &= \mathrm{Re}\Big\{\sum_{k=1}^{n} dY_2^k\ e^{ik\Omega_1 t}\Big\} \quad \vee \quad \dot{x}^2(t) = \mathrm{Re}\Big\{\sum_{k=1}^{n} dY_2^k\ e^{ik\Omega_1 t}\Big\} \\
x(t)|x^2(t)| &= \mathrm{Re}\Big\{\sum_{k=1}^{n} Y_3^k\ e^{ik\Omega_1 t}\Big\} \quad \vee \quad x^3(t) = \mathrm{Re}\Big\{\sum_{k=1}^{n} Y_3^k\ e^{ik\Omega_1 t}\Big\}
\end{aligned} \tag{3}$$

$$D(\Omega)\ X(\Omega) + c_2\ dY_2(\Omega) + k_3\ Y_3(\Omega) = F(\Omega), \tag{4}$$

Using N_{avg} spectral averages (obtained using e.g. a Hanning window) of signals $x(t)$, $f(t)$ and higher powers of $x(t)$ and $\dot{x}(t)$, Eq. (4) can be written in the form shown in Eqs. (5) and (6). For SDOF systems, matrices $\mathbf{X}$, $d\mathbf{Y}_2$, $\mathbf{Y}_3$ and $\mathbf{F}$ have size of $1 \times N_{avg}$. Moreover, Equations (5) and (6) are valid for every individual k-th frequency sample, $k \in \{1, \ldots, n\}$.

$$D(k\Omega_1)\ [X_1,\ \ldots,\ X_{N_{avg}}] + c_2\ [dY_{2,1},\ \ldots,\ dY_{2,N_{avg}}] + k_3\ [Y_{3,1},\ \ldots,\ Y_{3,N_{avg}}] = [F_1,\ \ldots,\ F_{N_{avg}}] \tag{5}$$

$$D(\Omega)\ \mathbf{X}(\Omega) + c_2\ d\mathbf{Y}_2(\Omega) + k_3\ \mathbf{Y}_3(\Omega) = \mathbf{F}(\Omega) \tag{6}$$

NIFO Algorithms

$\mathbf{H}_1$–based NIFO method (modified $\mathbf{H}_1$ algorithm)

The original NIFO estimator was first proposed in [1]. It can be obtained by rearranging Eq. (6) into the form presented in Eq. (7), where the quantity H is a Frequency Response Function ($H(\Omega) = D^{-1}(\Omega)$). The modified $\mathbf{H}_1$ algorithm is based on Eq. (8), which is obtained by right-multiplying Eq. (7) by the matrix $\begin{bmatrix}\mathbf{F}^H & -d\mathbf{Y}_2^H & -\mathbf{Y}_3^H\end{bmatrix}$. Note that an equation in the form of Eq. (8) can be written for every individual frequency.

$$\mathbf{X} = \begin{bmatrix} H & c_2H & k_3H \end{bmatrix} \begin{bmatrix} \mathbf{F} \\ -d\mathbf{Y}_2 \\ -\mathbf{Y}_3 \end{bmatrix} \tag{7}$$

$$\mathbf{X}\begin{bmatrix}\mathbf{F}^H & -d\mathbf{Y}_2^H & -\mathbf{Y}_3^H\end{bmatrix} = \begin{bmatrix}H & c_2H & k_3H\end{bmatrix}\begin{bmatrix}\mathbf{F} \\ -d\mathbf{Y}_2 \\ -\mathbf{Y}_3\end{bmatrix}\begin{bmatrix}\mathbf{F}^H & -d\mathbf{Y}_2^H & -\mathbf{Y}_3^H\end{bmatrix}$$

$$\underbrace{\begin{bmatrix}S_{XF} & -S_{XdY_2} & -S_{XdY_3}\end{bmatrix}}_{\mathbf{b}} = \underbrace{\begin{bmatrix}H & c_2H & k_3H\end{bmatrix}}_{\hat{\mathbf{x}}}\underbrace{\begin{bmatrix}S_{FF} & -S_{FdY_2} & -S_{FY_3} \\ & S_{dY_2dY_2} & S_{dY_2Y_3} \\ \textbf{Herm. Mtrx} & & S_{Y_3Y_3}\end{bmatrix}}_{\mathbf{A}} \tag{8}$$

The $\mathbf{H}_1$–based NIFO algorithm results in multiple systems of linear equations of the form $\mathbf{b} = \hat{\mathbf{x}}\mathbf{A}$ (each system corresponds to a different frequency sample). Matrix $\mathbf{A}$ is square and for problems of our interest it is usually non-singular, thus it might be possible to accurately estimate the frequency response function $H(\Omega)$ and parameters c_2 and k_3 through solving Eq. (8).

Note that the nonlinear parameters c_2 and k_3 were introduced in Eqs. (1) or (2) as *real* and *constant* numbers. However, they are computed as *complex* and possibly *frequency-dependent*, since some of the parameters in Eq. (8) are complex (as already mentioned above) and the system of equations is solved for each frequency sample separately.

$\mathbf{H}_2$–based NIFO method (modified $\mathbf{H}_2$ algorithm)

The $\mathbf{H}_2$–based NIFO algorithm was first presented in [2]. It is derived by adding additional pseudo-outputs to Eq. (7). These additional outputs, $\mathbf{X}_{nl,1}$ and $\mathbf{X}_{nl,2}$, correspond to the nonlinear terms in the EOM, as shown in Eq. (9). The modified $\mathbf{H}_2$ algorithm is based on the formula presented in Eq. (10). It can be obtained through right-multiplying Eq. (9) by matrix $\begin{bmatrix}\mathbf{X}^H & \mathbf{X}_{nl,1}^H & \mathbf{X}_{nl,2}^H\end{bmatrix}$. As shown in Eq. (10), the modification proposed in Eq. (9) is needed to overcome the issue of inverting a rectangular matrix. Moreover, due to the cubic stiffness and quadratic damping nonlinearities, we can write: $\mathbf{X}_{nl,1} = d\mathbf{Y}_2$ and $\mathbf{X}_{nl,2} = \mathbf{Y}_3$ and bring Eq. (10) to a form of Eq. (11). Detailed derivation of the modified $\mathbf{H}_2$ method is presented in [2].

$$\begin{bmatrix}\mathbf{X} \\ \mathbf{X}_{nl,1} \\ \mathbf{X}_{nl,2}\end{bmatrix} = \begin{bmatrix}H & c_2H & k_3H \\ & -1 & \\ & & -1\end{bmatrix}\begin{bmatrix}\mathbf{F} \\ -d\mathbf{Y}_2 \\ -\mathbf{Y}_3\end{bmatrix} \tag{9}$$

$$\begin{bmatrix}\mathbf{X} \\ \mathbf{X}_{nl,1} \\ \mathbf{X}_{nl,2}\end{bmatrix}\begin{bmatrix}\mathbf{X}^H & \mathbf{X}_{nl,1}^H & \mathbf{X}_{nl,2}^H\end{bmatrix} = \begin{bmatrix}H & c_2H & k_3H \\ & -1 & \\ & & -1\end{bmatrix}\begin{bmatrix}\mathbf{F} \\ -d\mathbf{Y}_2 \\ -\mathbf{Y}_3\end{bmatrix}\begin{bmatrix}\mathbf{X}^H & \mathbf{X}_{nl,1}^H & \mathbf{X}_{nl,2}^H\end{bmatrix}$$

$$\begin{bmatrix}S_{XX} & S_{XX_{nl,1}} & S_{XX_{nl,2}} \\ & S_{X_{nl,1}X_{nl,1}} & S_{X_{nl,1}X_{nl,2}} \\ \textbf{Herm. Mtrx} & & S_{X_{nl,2}X_{nl,2}}\end{bmatrix} = \begin{bmatrix}H & c_2H & k_3H \\ & -1 & \\ & & -1\end{bmatrix}\begin{bmatrix}S_{FX} & S_{FX_{nl,1}} & S_{FX_{nl,2}} \\ -S_{dY_2X} & -S_{dY_2X_{nl,1}} & -S_{dY_2X_{nl,2}} \\ -S_{Y_3X} & -S_{Y_3X_{nl,1}} & -S_{Y_3X_{nl,2}}\end{bmatrix} \tag{10}$$

$$\overbrace{\begin{bmatrix}S_{XX} & S_{XdX_2} & S_{XX_3} \\ & S_{dX_2dX_2} & S_{dX_2X_3} \\ \textbf{Herm. Mtrx} & & S_{X_3X_3}\end{bmatrix}}^{\mathbf{U}} = \overbrace{\begin{bmatrix}H & c_2H & k_3H \\ & -1 & \\ & & -1\end{bmatrix}}^{\hat{\mathbf{X}}}\overbrace{\begin{bmatrix}S_{FX} & S_{FdX_2} & S_{FX_3} \\ -S_{dY_2X} & -S_{dY_2dX_2} & -S_{dY_2X_3} \\ -S_{Y_3X} & & -S_{Y_3X_3}\end{bmatrix}}^{\mathbf{B}} \tag{11}$$

Hermitian Sub-matrix

Summary of the modified $\mathbf{H}_2$ algorithm derivation is analogous to the one presented in section on its twin algorithm – $\mathbf{H}_1$–based NIFO. Nevertheless, one additional comment might be worth noting. Namely, the rows of matrices $\mathbf{B}$ and $\mathbf{U}$ (ranging from the 2nd to the last) are almost the same. The rows of matrix $\mathbf{B}$ are rows of $\mathbf{U}$, but multiplied by -1. This simple observation can be used to save time spent on algorithm implementation. Using MATLAB notation we could write:

```
B(2:end, :)  = -U(2:end, :);
```

Nonlinear Identification through eXtended Outputs Algorithms

$\mathbf{H}_1$–based NIXO method

The NIXO methods seek to form a larger linear system in which frequency independent parameters can be enforced. We begin by right-multiplying Eq. (6) by $\mathbf{F}^H$ to obtain Eq. (12), which is valid for every individual frequency line. Hence, it is possible to express each of these equations the matrix form shown in Eq. (13). Note that the frequency sample number is indicated in the quantities' sub- or superscripts, e.g. $S_{XF}(\Omega_i) = S^i_{XF}$ or $D(\Omega_i) = D_i$.

$$\begin{aligned} D(\Omega)\ \mathbf{X}\mathbf{F}^H + c_2\ d\mathbf{Y}_2\mathbf{F}^H + k_3\ \mathbf{Y}_3\mathbf{F}^H &= \mathbf{F}\mathbf{F}^H \\ D(\Omega)\ S_{XF} + c_2\ S_{dY_2F} + k_3\ S_{Y_3F} &= S_{FF} \end{aligned} \tag{12}$$

$$\underbrace{\begin{bmatrix} S^1_{XF} & & & S^1_{dY_2F} & S^1_{Y_3F} \\ & \ddots & & \vdots & \vdots \\ & & S^n_{XF} & S^n_{dY_2F} & S^n_{Y_3F} \end{bmatrix}}_{\mathbf{S}^{H1}_{XF}} \begin{bmatrix} D_1 \\ \vdots \\ D_n \\ c_2 \\ k_3 \end{bmatrix} = \underbrace{\begin{bmatrix} S^1_{FF} \\ \vdots \\ S^n_{FF} \end{bmatrix}}_{\mathbf{S}^{H1}_{FF}}, \tag{13}$$

where n stands for the number of frequency samples.

Unfortunately, Eq. (13) cannot simply be solved by inverting the matrix on the left because there are more unknowns than equations. To be more precise we obtained $2n$ equations and $2n + p_{damp} + p_{stiff}$ unknowns, since some of the parameters in Eq. (13) are complex numbers in general. Naturally, p_{damp} and p_{stiff} represent herein the number of the nonlinear damping and stiffness terms in the equation of motion (1) or (2). In this particular example $p_{damp} = 1$ and $p_{stiff} = 1$.

If the solution of the underdetermined system of equations exists – it is not unique. This can lead to inaccuracies in the parameter estimation. The main concept behind the new $\boldsymbol{H}_1$ *Nonlinear Identification through eXtended Outputs* ($\mathbf{H}_1$-NIXO) estimator is to overcome this indeterminacy by providing input and output data sets collected in vibration tests where the system oscillates at multiple different amplitudes. Such data can be used to increase the the number of equations in Eq. (13) while keeping the number of unknowns fixed. The idea originates from two observations:

1. Parameters from Eqs. (1, 2), namely $m,\ c,\ k$ as well as c_2 and k_3, define the mechanical system regardless of the excitation type

2. Nonlinear response of the system occurs when it oscillates at large enough amplitudes. Hence, if the set of equations (13) is put together, *separately*, for mechanical system oscillating at, say, *two* different amplitudes – it might be possible (due to the nonlinearity) that these $4n$ *real* equations will be linearly independent. Since the number of *real* unknowns ($2n + p_{damp} + p_{stiff}$) is kept constant - then this new (stacked) system of equations becomes overdetermined and thus will typically have a unique solution[1].

To define the algorithm mathematically, consider the same mechanical system subjected, separately, to multiple forcing functions. This forcing functions have to be chosen such that they cause a response at multiple different displacement magnitudes (e.g. they could be chosen as multiple swept sines of different forcing levels), see Eq. (14).

$$\begin{cases} m\ddot{x} + c\dot{x} + kx + c_2\dot{x}|\dot{x}| + k_3x^3 &= f_I(t) \\ m\ddot{x} + c\dot{x} + kx + c_2\dot{x}|\dot{x}| + k_3x^3 &= f_{II}(t) \\ & \vdots \\ m\ddot{x} + c\dot{x} + kx + c_2\dot{x}|\dot{x}| + k_3x^3 &= f_r(t) \end{cases}, \tag{14}$$

where r is the number of different forcing functions used to excite the mechanical system.

[1] One cannot guarantee that the new equations will be linearly independent of those already provided, but if the nonlinearities are amplitude dependent and sufficiently different amplitudes are used then this is likely to be the case.

If we repeat the derivation presented above in this section we end up with r-times the number of equations presented in Eq. (13) and an unchanged number of unknowns, with the final form given in Eq. (15).

$$\begin{bmatrix} \mathbf{S}^{H1}_{XF,I} \\ \mathbf{S}^{H1}_{XF,II} \\ \vdots \\ \mathbf{S}^{H1}_{XF,r} \end{bmatrix} \begin{bmatrix} D_1 \\ \vdots \\ D_n \\ c_2 \\ k_3 \end{bmatrix} = \begin{bmatrix} \mathbf{S}^{H1}_{FF,I} \\ \mathbf{S}^{H1}_{FF,II} \\ \vdots \\ \mathbf{S}^{H1}_{FF,r} \end{bmatrix} \tag{15}$$

Since some of the parameters in Eq. (15) are complex, the estimates of c_2 and k_3 are not guaranteed to be real numbers. To overcome this issue, the real and imaginary parts of the unknowns should be estimated separately so that one can force the nonlinear parameter values to be real. To do so, Eq. (15) should be brought to its equivalent form presented in Eq. (16). The system of derived equations (16) is now overdetermined and the unknown parameters can be estimated by solving a linear least squares problem.

$$\begin{bmatrix}
Re\{S^1_{XF,I}\} & -Im\{S^1_{XF,I}\} & & & & & Re\{S^1_{dY_2F,I}\} & Re\{S^1_{Y_3F,I}\} \\
Im\{S^1_{XF,I}\} & Re\{S^1_{XF,I}\} & & & & & Im\{S^1_{dY_2F,I}\} & Im\{S^1_{Y_3F,I}\} \\
 & & \ddots & & & & \vdots & \vdots \\
 & & & Re\{S^n_{XF,I}\} & -Im\{S^n_{XF,I}\} & & Re\{S^n_{dY_2F,I}\} & Re\{S^n_{Y_3F,I}\} \\
 & & & Im\{S^n_{XF,I}\} & Re\{S^n_{XF,I}\} & & Im\{S^n_{dY_2F,I}\} & Im\{S^n_{Y_3F,I}\} \\
Re\{S^1_{XF,II}\} & -Im\{S^1_{XF,II}\} & & & & & Re\{S^1_{dY_2F,II}\} & Re\{S^1_{Y_3F,II}\} \\
Im\{S^1_{XF,II}\} & Re\{S^1_{XF,II}\} & & & & & Im\{S^1_{dY_2F,II}\} & Im\{S^1_{Y_3F,II}\} \\
 & & \ddots & & & & \vdots & \vdots \\
 & & & Re\{S^n_{XF,II}\} & -Im\{S^n_{XF,II}\} & & Re\{S^n_{dY_2F,II}\} & Re\{S^n_{Y_3F,II}\} \\
 & & & Im\{S^n_{XF,II}\} & Re\{S^n_{XF,II}\} & & Im\{S^n_{dY_2F,II}\} & Im\{S^n_{Y_3F,II}\} \\
 & & \vdots & & & & \vdots & \vdots \\
Re\{S^1_{XF,r}\} & -Im\{S^1_{XF,r}\} & & & & & Re\{S^1_{dY_2F,r}\} & Re\{S^1_{Y_3F,r}\} \\
Im\{S^1_{XF,r}\} & Re\{S^1_{XF,r}\} & & & & & Im\{S^1_{dY_2F,r}\} & Im\{S^1_{Y_3F,r}\} \\
 & & \ddots & & & & \vdots & \vdots \\
 & & & Re\{S^n_{XF,r}\} & -Im\{S^n_{XF,r}\} & & Re\{S^n_{dY_2F,r}\} & Re\{S^n_{Y_3F,r}\} \\
 & & & Im\{S^n_{XF,r}\} & Re\{S^n_{XF,r}\} & & Im\{S^n_{dY_2F,r}\} & Im\{S^n_{Y_3F,r}\}
\end{bmatrix}
\begin{bmatrix} Re\{D_1\} \\ Im\{D_1\} \\ \vdots \\ Re\{D_n\} \\ Im\{D_n\} \\ c_2 \\ k_3 \end{bmatrix} =
\begin{bmatrix}
Re\{S^1_{FF,I}\} \\ Im\{S^1_{FF,I}\} \\ \vdots \\ Re\{S^n_{FF,I}\} \\ Im\{S^n_{FF,I}\} \\
Re\{S^1_{FF,II}\} \\ Im\{S^1_{FF,II}\} \\ \vdots \\ Re\{S^n_{FF,II}\} \\ Im\{S^n_{FF,II}\} \\
\vdots \\
Re\{S^1_{FF,r}\} \\ Im\{S^1_{FF,r}\} \\ \vdots \\ Re\{S^n_{FF,r}\} \\ Im\{S^n_{FF,r}\}
\end{bmatrix} \tag{16}$$

$\mathbf{H}_2$–based NIXO method

To identify the nonlinear mechanical system using the new ***H_2*** *Nonlinear Identification through eXtended Outputs* ($\mathbf{H}_2$-NIXO) estimator, bring Eq. (6) to a form of Eq. (17) and right-multiply it by matrix $\begin{bmatrix}\mathbf{X}^H & d\mathbf{Y}_2^H & \mathbf{Y}_3^H\end{bmatrix}$.

Equation (18) is valid for every individual frequency sample. Thus, it is possible to express each of these equations in a matrix form shown in Eq. (19). As before the frequency sample number is indicated in the quantities' sub- or superscripts, e.g. $S_{XX}(\Omega_i) = S^i_{XX}$ or $D(\Omega_i) = D_i$.

$$\begin{bmatrix} D(\Omega) & c_2 & k_3 \end{bmatrix} \begin{bmatrix} \mathbf{X} \\ d\mathbf{Y}_2 \\ \mathbf{Y}_3 \end{bmatrix} = \mathbf{F} \tag{17}$$

$$\begin{bmatrix} D(\Omega) & c_2 & k_3 \end{bmatrix} \begin{bmatrix} \mathbf{X} \\ d\mathbf{Y}_2 \\ \mathbf{Y}_3 \end{bmatrix} \begin{bmatrix} \mathbf{X}^H & d\mathbf{Y}_2^H & \mathbf{Y}_3^H \end{bmatrix} = \mathbf{F} \begin{bmatrix} \mathbf{X}^H & d\mathbf{Y}_2^H & \mathbf{Y}_3^H \end{bmatrix}$$

$$\begin{bmatrix} D(\Omega) & c_2 & k_3 \end{bmatrix} \begin{bmatrix} S_{XX} & S_{XdY_2} & S_{XY_3} \\ \textbf{Herm.} & S_{dY_2dY_2} & S_{dY_2Y_3} \\ & \textbf{Mtrx} & S_{Y_3Y_3} \end{bmatrix} = \begin{bmatrix} S_{FX} & S_{FdY_2} & S_{FY_3} \end{bmatrix} \Big| (\ )^H \Longrightarrow$$

$$\Longrightarrow \begin{bmatrix} S_{XX} & S_{XdY_2} & S_{XY_3} \\ \textbf{Herm.} & S_{dY_2dY_2} & S_{dY_2Y_3} \\ & \textbf{Mtrx} & S_{Y_3Y_3} \end{bmatrix} \begin{bmatrix} D^H(\Omega) \\ c_2 \\ k_3 \end{bmatrix} = \begin{bmatrix} S_{XF} \\ S_{dY_2F} \\ S_{Y_3F} \end{bmatrix} \tag{18}$$

$$\begin{bmatrix} S^1_{XX} & & & S^1_{XdY_2} & S^1_{XY_3} \\ & \ddots & & \vdots & \vdots \\ & & S^n_{XX} & S^n_{XdY_2} & S^n_{XY_3} \\ S^1_{dY_2X} & & & S^1_{dY_2dY_2} & S^1_{dY_2Y_3} \\ & \ddots & & \vdots & \vdots \\ & & S^n_{dY_2X} & S^n_{dY_2dY_2} & S^n_{dY_2Y_3} \\ S^1_{Y_3X} & & & S^1_{Y_3dY_2} & S^1_{Y_3Y_3} \\ & \ddots & & \vdots & \vdots \\ & & S^n_{Y_3X} & S^n_{Y_3dY_2} & S^n_{Y_3Y_3} \end{bmatrix} \begin{bmatrix} D^H_1 \\ \vdots \\ D^H_n \\ c_2 \\ k_3 \end{bmatrix} = \begin{bmatrix} S^1_{XF} \\ \vdots \\ S^n_{XF} \\ S^1_{dY_2F} \\ \vdots \\ S^n_{dY_2F} \\ S^1_{Y_3F} \\ \vdots \\ S^n_{Y_3F} \end{bmatrix} \tag{19}$$

To assure that the nonlinear parameters c_2 and k_3 are estimated as real numbers, the problem stated in Eq. (19) should be separated into real and imaginary parts, as illustrated in the previous section. As with the prior algorithm, with $\mathbf{H}_2$-NIXO we then obtain a linear least squares problem to solve to estimate the nonlinear system parameters.

Nonlinear Identification through eXtended Outputs Algorithms with Linear Data Provided

Two new nonlinear estimators are presented in the previous section. In addition to finding the values of the parameters describing the nonlinearities, the algorithms also return estimates of the linear Frequency Response Function (FRF). Since linear experimental vibration analysis can be considered today as well–established, the linear FRF values could possibly be treated as known (i.e. they could be obtained in a separate test where the structure vibrates at low enough amplitude). With this assumption, we could modify the final equations obtained in the previous sections by bringing the FRF terms to the RHS vector of known values. This simple observation reduces the number of unknowns – now the only unknown parameters are c_2 and k_3. This also significantly reduces sizes of matrices in Eqs. (15), (16) and (19), which makes the algorithms more efficient from the computational viewpoint. This is elaborated below.

$\mathbf{H}_1$-NIXO with Linear Data Provided

If the linear Frequency Response Function is known then Eq. (15) can be brought to the form shown in Eq. (20) where quantities corresponding to D_j's are now placed in the RHS vector of known values. Note also that collecting data from multiple vibration tests is no longer needed. The system of equations (20) is most likely overdetermined, since the number of frequency samples ($n \sim 1000$) is usually larger than the number of unknown polynomial terms ($p_{dapmp},\ p_{stiff} \sim 10$). In case of $p_{dapmp} + p_{stiff} > n$ (which is possible but unlikely), then the number of equations can be populated by providing data collected in vibration tests where the mechanical system oscillates at multiple different amplitudes (as explained in one of the previous sections).

$$\underbrace{\begin{bmatrix} S^1_{dY_2F} & S^1_{Y_3F} \\ \vdots & \vdots \\ S^n_{dY_2F} & S^n_{Y_3F} \end{bmatrix}}_{\mathbf{A}_1} \begin{bmatrix} c_2 \\ k_3 \end{bmatrix} = \underbrace{\begin{bmatrix} S^1_{FF} - S^1_{XF} D_1 \\ \vdots \\ S^n_{FF} - S^n_{XF} D_n \end{bmatrix}}_{\mathbf{b}_1} \tag{20}$$

To enforce the algorithm to estimate the nonlinear parameters c_2 and k_3 as real numbers, Eq. (20) should be brought to its equivalent real form shown in Eq. (21), where matrix A_1 and vector b_1 are defined in Eq. (20).

$$\begin{bmatrix} Re\{\mathbf{A}_1\} \\ Im\{\mathbf{A}_1\} \end{bmatrix} \begin{bmatrix} c_2 \\ k_3 \end{bmatrix} = \begin{bmatrix} Re\{\mathbf{b}_1\} \\ Im\{\mathbf{b}_1\} \end{bmatrix} \tag{21}$$

$\mathbf{H}_2$-NIXO with Linear Data Provided

The derivation for this algorithm is analogous to that in the previous section. If the linear Frequency Response Function is known then Eq. (19) can be brought to the form shown in Eq. (22) where quantities corresponding to D_j's are now placed in the vector on the RHS. The system of equations (22) is always overdetermined.

$$\underbrace{\begin{bmatrix} S^1_{XdY_2} & S^1_{XY_3} \\ \vdots & \vdots \\ S^n_{XdY_2} & S^n_{XY_3} \\ S^1_{dY_2dY_2} & S^1_{dY_2Y_3} \\ \vdots & \vdots \\ S^n_{dY_2dY_2} & S^n_{dY_2Y_3} \\ S^1_{Y_3dY_2} & S^1_{Y_3Y_3} \\ \vdots & \vdots \\ S^n_{Y_3dY_2} & S^n_{Y_3Y_3} \end{bmatrix}}_{\mathbf{A}_2} \begin{bmatrix} c_2 \\ k_3 \end{bmatrix} = \underbrace{\begin{bmatrix} S^1_{XF} - S^1_{XX} D^H_1 \\ \vdots \\ S^n_{XF} - S^n_{XX} D^H_n \\ S^1_{dY_2F} - S^1_{dY_2X} D^H_1 \\ \vdots \\ S^n_{dY_2F} - S^n_{dY_2X} D^H_n \\ S^1_{Y_3F} - S^1_{Y_3X} D^H_1 \\ \vdots \\ S^n_{Y_3F} - S^n_{Y_3X} D^H_n \end{bmatrix}}_{\mathbf{b}_2} \tag{22}$$

To enforce the algorithm to estimate the nonlinear parameters c_2 and k_3 as real numbers, Eq. (22) should be brought to its equivalent form presented in Eq. (21), where $\mathbf{A}_1$ and $\mathbf{b}_1$ are obviously replaced with $\mathbf{A}_2$ and $\mathbf{b}_2$, respectively. Matrix $\mathbf{A}_2$ and vector $\mathbf{b}_2$ are defined in Eq. (22).

Case Study

Mechanical System Description

The algorithms are evaluated using input and output signals collected during simulated experiments of a mechanical system described by the Duffing equation (23). Values for the parameters were proposed in [1] and are given in Tab. 1. Auto- and cross-spectra in every case study presented are obtained by applying 25-second-long Hanning windows with 51% of overlap.

$$m\ddot{x} + c\dot{x} + kx + k_3x^3 = f(t) \tag{23}$$

Tab. 1: Parameters describing SDOF mechanical system with cubic stiffness nonlinearity.

$m\ \left[\mathrm{kg}\right]$	$c\ \left[\frac{\mathrm{N\ s}}{\mathrm{m}}\right]$	$k\ \left[\frac{\mathrm{N}}{\mathrm{m}}\right]$	$k_3\ \left[\frac{\mathrm{N}}{\mathrm{m}^3}\right]$
1	4	10^3	10^5

Forcing Signals Description

Input and output signals are generated by exciting the structure with two types of forcing functions:

Swept Cosine Forcing Signal

$$f(t) = F\cos(\Omega(t)\ t) \qquad \Omega(t) = \Omega_{st} + \frac{\Omega_{end} - \Omega_{st}}{t_{end} - t_{st}}(t - t_{st}) \qquad t \in [t_{st},\ t_{end}] \tag{24}$$

Broad-Band Burst Random Forcing Signal

$$f(t) = F\ BurstRand(t) \qquad t \in [t_{st},\ t_{end}] \tag{25}$$

Case Study 1. System Identification with Model Function Known À Priori

The NIXO and NIFO methods are first used to identify the mechanical system (23) with the model function known beforehand. Forcing signals (both swept cosine and burst random) are defined in Tabs. 2 and Tab. 3. The results obtained are presented in Tables 4 to 7 and discussed briefly at the end of this subsection.

Tab. 2: Values of parameters characteristic to swept cosine and burst random forcing functions.

	Ω_{st} [Hz]	Ω_{end} [Hz]	t_{st} [s]	t_{end} [s]
Swept Cosine:	0.01	15	0	1500

	t_{st} [s]	t_{end} [s]	Δt [s]	Burst Start	Burst End
Burst Random:	0	512.5	0.01	0%	100%

Tab. 3: Values of parameters shared by swept cosine and burst random forcing functions. Force amplitudes expressed in newtons, frequencies expressed in hertz.

Signal Type	F_I or F	F_{II}	DF	FO	Ω_1^{filt}	Ω_2^{filt}	Ω_1^{spect}	Ω_2^{spect}	I/O Signals	Results
Swept Cosine	5.0	0.1	-	-	-	-	0.3	15	Tab. 4	Tab. 5
Burst Random	10.0	0.1	2	8	0.3	15	0.3	15	Tab. 6	Tab. 7

DF – Decimation Factor

FO – Butterworth Filter Order

Ω^{filt} – cut-off frequency; Ω_1^{filt} and Ω_2^{filt} are lower and upper cut-off frequencies, respectively

Ω^{spect} – auto- and cross-spectra are computed for frequency range (Ω_1^{spect}, Ω_2^{spect}).

Tab. 4: Case study with Swept Cosine used as a forcing function. Input/Output Signals.

Signal Type	F_I or F	F_{II}	DF	FO	Ω_1^{filt}	Ω_2^{filt}	Ω_1^{spect}	Ω_2^{spect}
Swept Cosine	5.000	0.100	-	-	-	-	0.3	15

Signal	Time domain	Freq. domain
$f(t)$	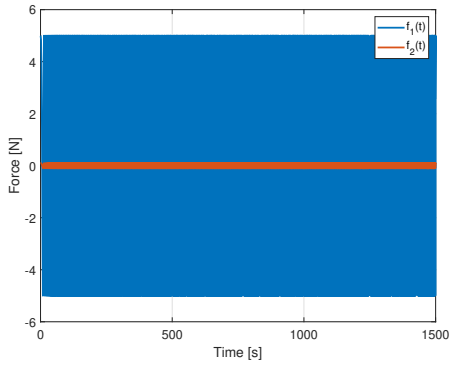	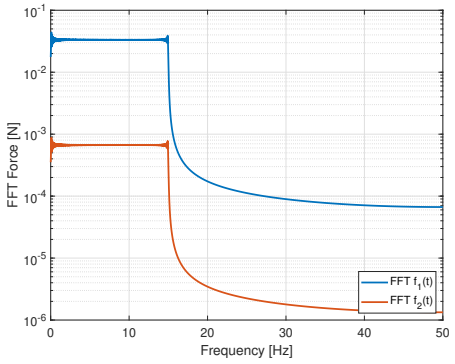
$x(t)$	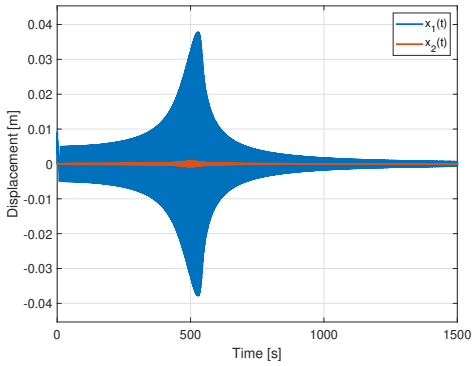	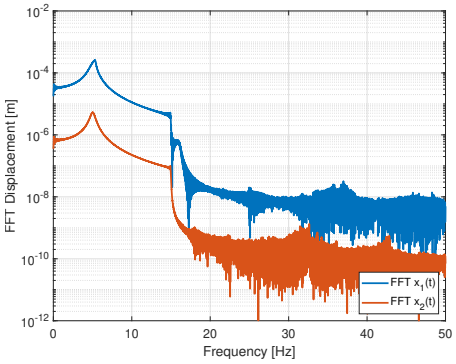
$v(t)$	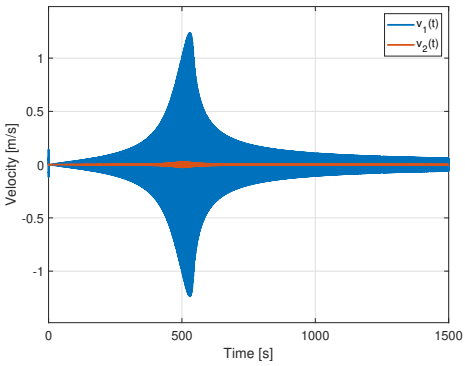	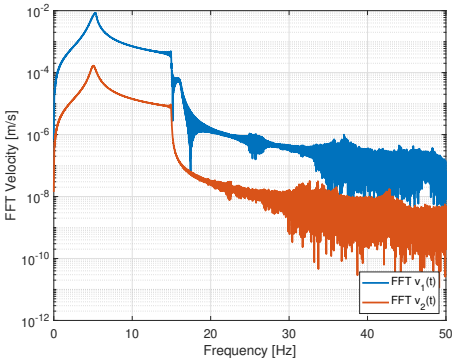

Tab. 5: Case study with Swept Cosine used as a forcing function. Results.

Signal Type	F_I or F	F_{II}	DF	FO	Ω_1^{filt}	Ω_2^{filt}	Ω_1^{spect}	Ω_2^{spect}
Swept Cosine	5.000	0.100	-	-	-	-	0.3	15

Method	Linear FRF estimate	Nonlin. param. estimates (rel. error)
$\mathbf{H}_1$-NIFO	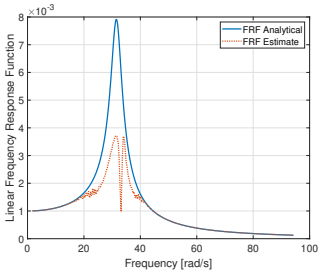	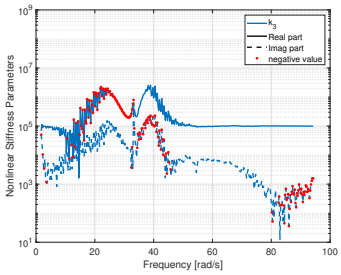
$\mathbf{H}_2$-NIFO	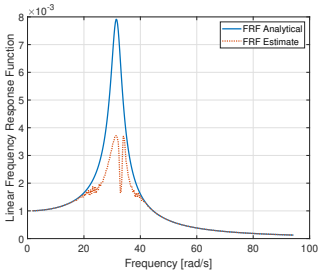	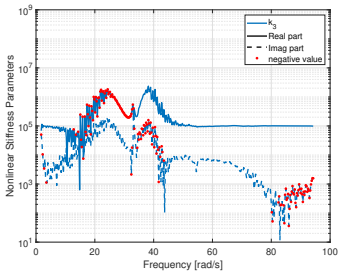
$\mathbf{H}_1$-NIXO	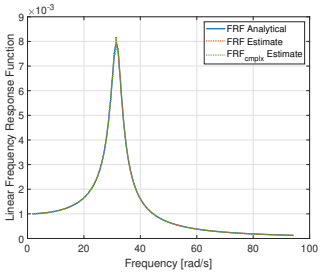	$k_3 = 9.917e+04\ (0.83\%)$ $k_{3,cmplx} = 9.917e+04\ -\ i2.893e+02$
$\mathbf{H}_2$-NIXO	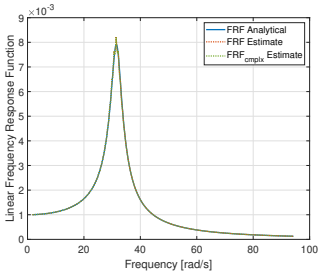	$k_3 = 1.040e+05\ (4.01\%)$ $k_{3,cmplx} = 1.040e+05\ -\ i5.453e+02$
$\mathbf{H}_1$-NIXO with lin. data provided	$\times$	$k_3 = 9.991e+04\ (0.09\%)$ $k_{3,cmplx} = 9.991e+04\ +\ i5.840e+02$
$\mathbf{H}_2$-NIXO with lin. data provided	$\times$	$k_3 = 9.981e+04\ (0.19\%)$ $k_{3,cmplx} = 9.981e+04\ -\ i4.633e+01$

Tab. 6: Case study with Burst Random forcing function. Input/Output Signals.

Signal Type	F_I or F	F_{II}	DF	FO	Ω_1^{filt}	Ω_2^{filt}	Ω_1^{spect}	Ω_2^{spect}
Burst Random	10.000	0.100	2	8	0.3	15	0.3	15

Signal	Time domain	Freq. domain
$f_I(t)$	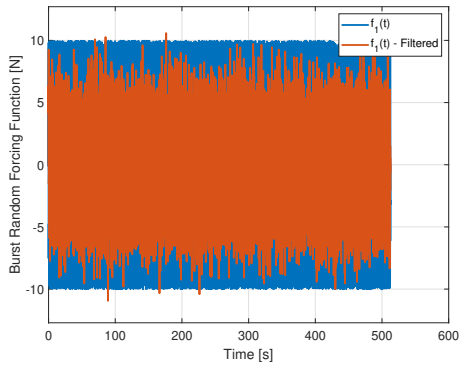	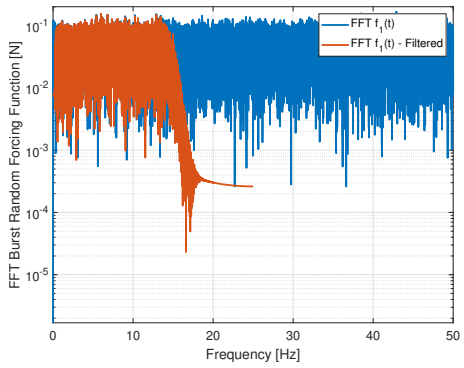
$f_{II}(t)$	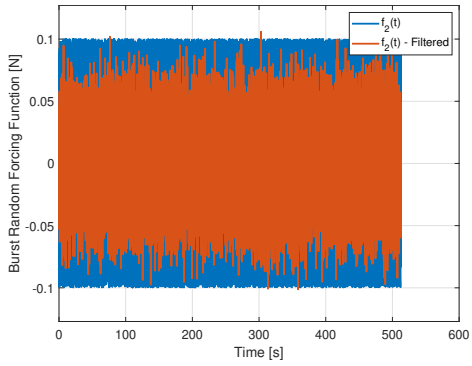	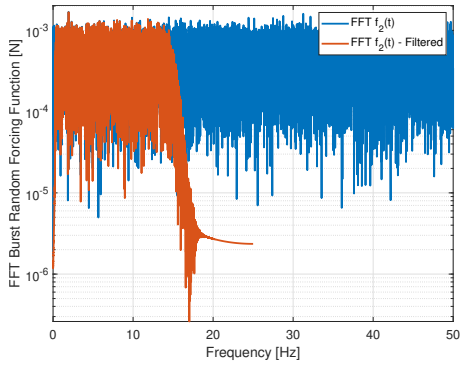
$x(t)$	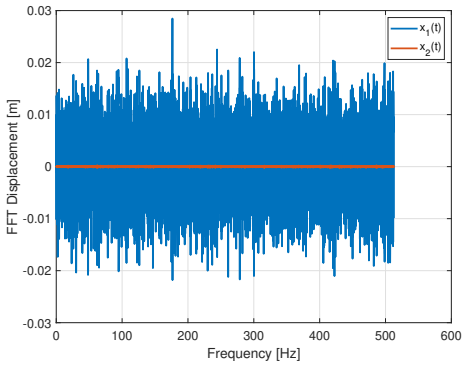	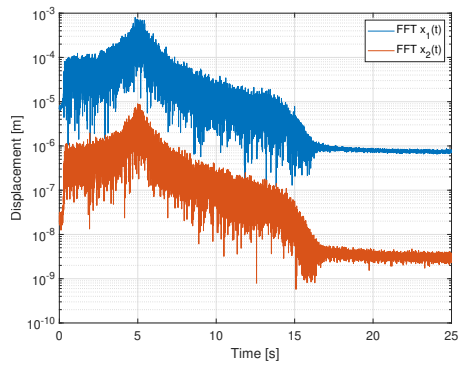
$v(t)$	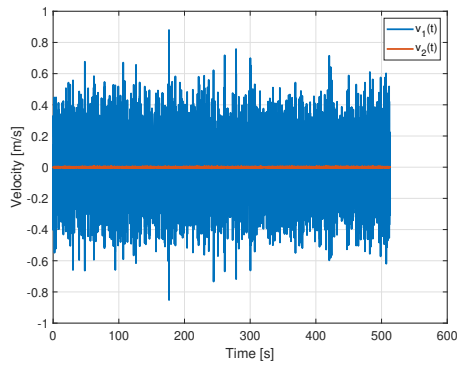	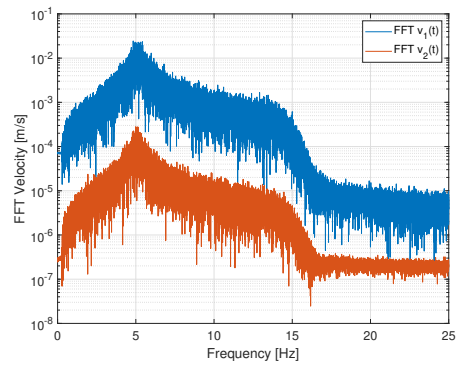

Tab. 7: Case study with Burst Random forcing function. Results.

Signal Type	F_I or F	F_{II}	DF	FO	Ω_1^{filt}	Ω_2^{filt}	Ω_1^{spect}	Ω_2^{spect}
Burst Random	10.000	0.100	2	8	0.3	15	0.3	15

Method	Linear FRF estimate	Nonlin. param. estimates (rel. error)
$\mathbf{H}_1$-NIFO	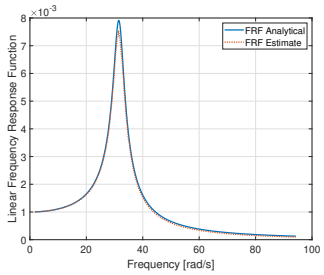	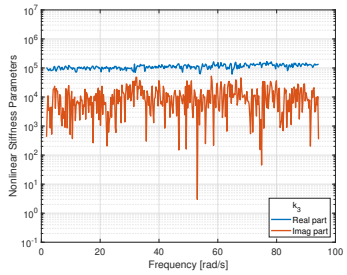
$\mathbf{H}_2$-NIFO	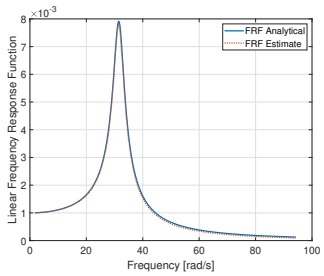	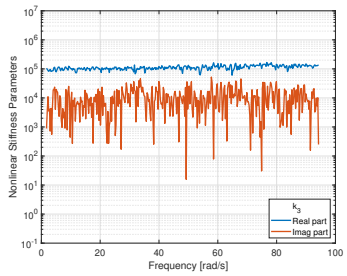
$\mathbf{H}_1$-NIXO	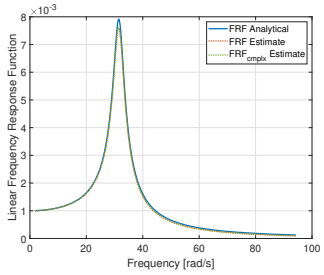	$k_3 = 9.914e+04$ (0.86%) $k_{3,cmplx} = 9.914e+04 \; + \; i1.813e+03$
$\mathbf{H}_2$-NIXO	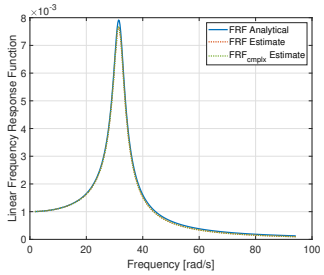	$k_3 = 1.047e+05$ (4.73%) $k_{3,cmplx} = 1.047e+05 \; + \; i5.614e+03$
$\mathbf{H}_1$-NIXO with lin. data provided	×	$k_3 = 4.681e+04$ (53.19%) $k_{3,cmplx} = 4.681e+04 \; + \; i4.682e+04$
$\mathbf{H}_2$-NIXO with lin. data provided	×	$k_3 = 9.880e+04$ (1.20%) $k_{3,cmplx} = 9.880e+04 \; + \; i4.117e+04$

Comments to Case Study 1

1. In the case studies explored here, the NIFO methods failed to estimate the linear frequency response function when the input signal was swept cosine. However, if the system was excited with a burst random signal then NIFO estimated the FRF of the underlying linear system to a satisfactory extent. The NIXO methods, on the other hand, succeed in finding accurate enough estimates of the linear FRF regardless of the excitation type.

2. The NIFO algorithms returned accurate k_3 values away from the resonant frequency, while in the vicinity of the linear resonance their estimations were wildly erroneous. The NIXO methods return cubic stiffness parameter as a single *frequency-independent* value. Every NIXO algorithm succeeded in estimating k_3 to a satisfactory extent except for $\mathbf{H}_1$-NIXO–LDP. However, the accuracy of that method can be increased if data for higher excitation amplitudes is included (as shown in [5]).

3. It is worth noting that (for the NIXO and NIXO–LDP algorithms) the real part of k_3 found as a complex number matches the value of the cubic nonlinear parameter estimated as a real number. Moreover, the real part of k_3 is usually an accurate estimate when the imaginary part is found as a much smaller number. For example, the results obtained with the NIFO algorithms (with swept cosine used as the excitation) show that for off-resonant frequencies $Im\{k_3\}$ was much smaller than $Re\{k_3\}$. Thus, when an accurate parameter was found it typically was predominantly real. Additionally, this observations can be used as one of the decision criteria in the black-box system identification .

Case Study 2(a). Black-box System Identification – Impact of the Polynomial Degree

In this section, we propose a strategy to utilize the NIXO approaches to identify a single degree of freedom mechanical system of unknown nonlinearity. The algorithms are tested to estimate the parameters of Eq. (23) presented in Tab. 1. The model function used in the estimation process is given in Eq. (26).

Multiple tests, with different values of polynomial degree p and unknown k_i parameters ($i \in \{2, \ldots, p\}$), were conducted. A swept cosine forcing function, defined in Tabs. 2, 3 and presented in Tab. 4, was used as the input signal. The results obtained for the case where $p = 6$ are presented in Tab. 8.

$$m\ddot{x} + c\dot{x} + kx + k_2 x|x| + k_3 x^3 + \cdots + k_p x|x|^{p-1} = f(t) \tag{26}$$

The outcomes from this case study, obtained using NIXO methods, show that the cubic nonlinearity is most likely dominant in the mechanical system's response. Note that the cubic nonlinear stiffness term turned out to be the most significant for the identification with a polynomial of sixth degree (see e.g. the last column in Tab. 8). The results obtained with NIFO seem to be inconclusive.

Black-box system identification conducted for the remaining values of p ($p \in \{2, 3, \ldots, 9\}/\{6\}$) is presented in [6]. It shows similar outcomes for the identification with a polynomial of up to a sixth degree. The analyses conducted for polynomials of degree higher than 6 gave unclear results for both NIXO and NIFO algorithms. Hence, this approach would be limited to smaller numbers of polynomial terms. To explore this further, a second analysis was conducted. This time, the model function consisted of a cubic term and one additional nonlinear stiffness term only. The description and results obtained in this case study are presented in the next subsection.

Tab. 8: Degree of stiffness polynomial: 6. Black (red) border around the bars indicates positive (negative) value.

	Linear FRF estimate	Nonlin. param. estimates	Nonlin. terms FFT ($x(t)$ – output signal)
$\mathbf{H}_1$-NIFO	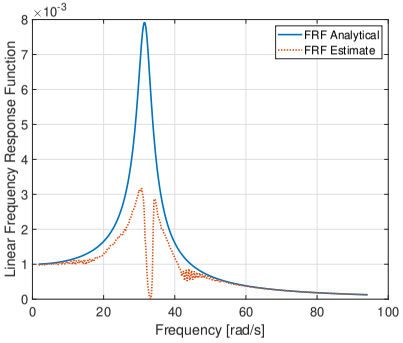	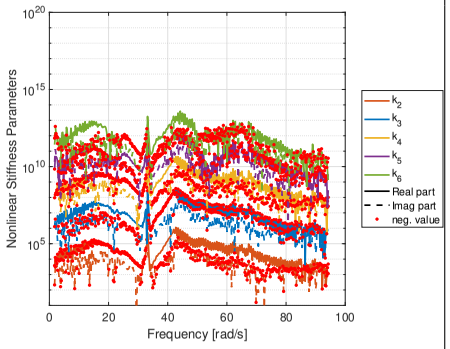	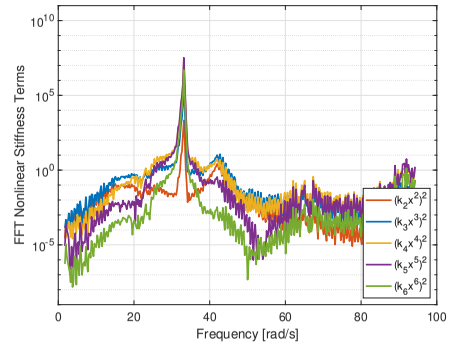
$\mathbf{H}_2$-NIFO	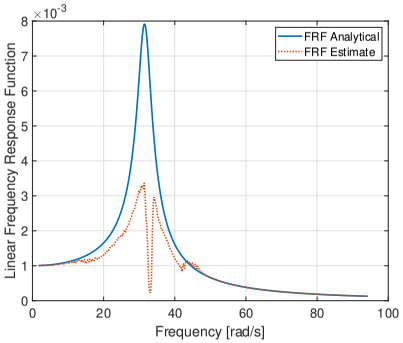	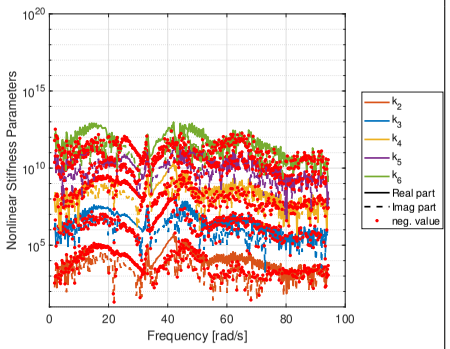	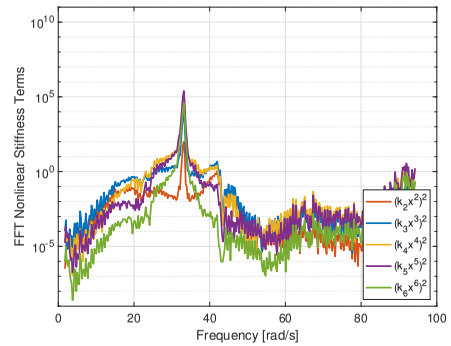
$\mathbf{H}_1$-NIXO	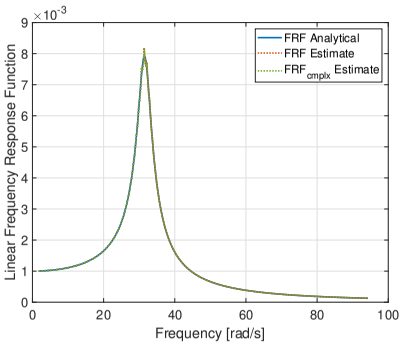	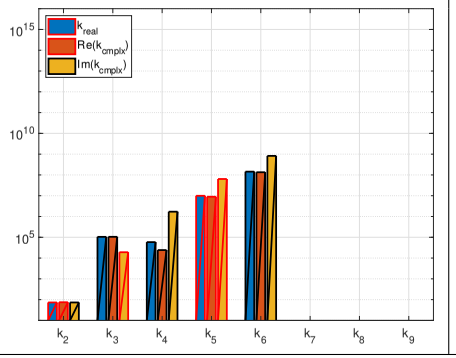	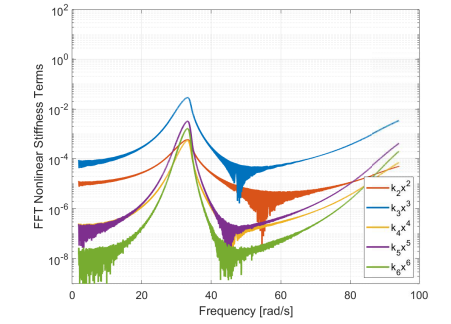

	Linear FRF estimate	Nonlin. param. estimates	Nonlin. terms FFT ($x(t)$ – output signal)
$\mathbf{H}_2$-NIXO	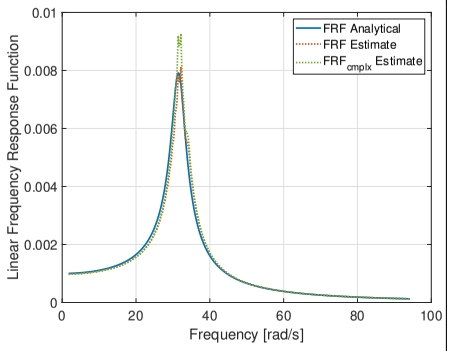	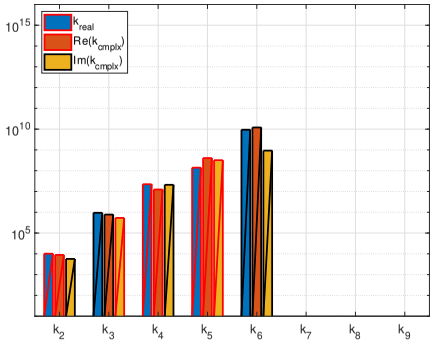	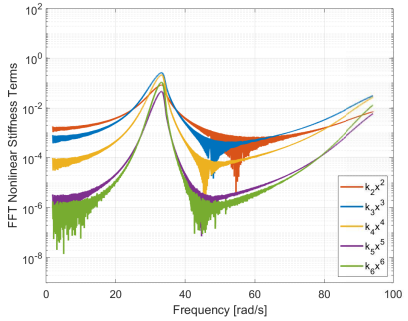
$\mathbf{H}_1$-NIXO WLDP	×	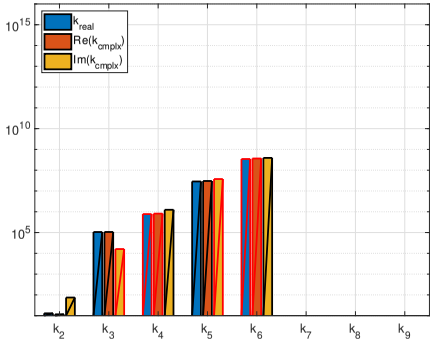	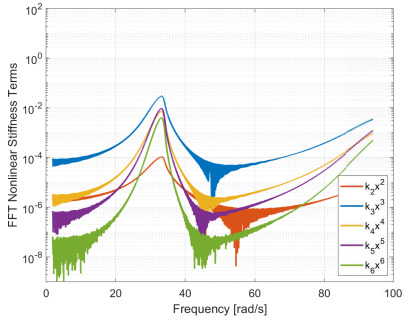
$\mathbf{H}_2$-NIXO WLDP	×	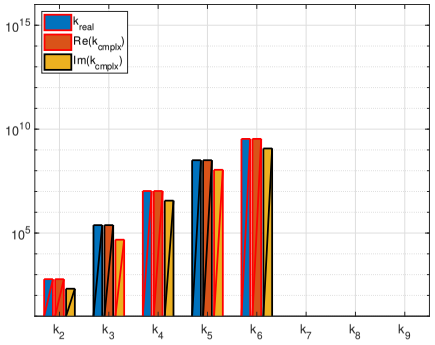	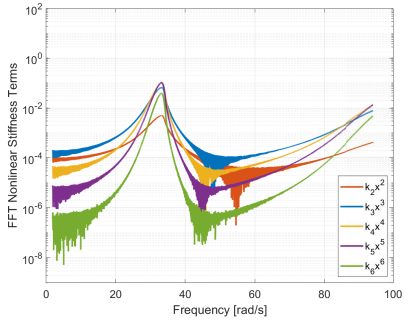

Case Study 2(b). Black-box System Identification – Impact of the Additional Polynomial Term

In the previous section, the results obtained correctly revealed that the stiffness nonlinearity in the mechanical system was most likely cubic. That term was dominant when the model function was a polynomial of up to sixth degree. However, when the model function (26) was assumed to be a polynomial of higher degree, the results did not give any insight into which nonlinear terms were dominant and which terms could be eliminated from the model function (for details see [6]).

In this section, the results obtained using Eq. (27) as a model function are presented. This function assumes that the nonlinearity in the system consists of a cubic term and one additional term only.

$$m\ddot{x} + c\dot{x} + kx + k_3x^3 + k_rx|x|^{p-1} = f(t) \tag{27}$$

The mechanical system is again subjected to the swept cosine excitation defined previously. Table 9 shows the outcomes from the analysis for additional term power $p = 9$. Results obtained for the remaining powers, namely $p \in \{7, 8\}$ can be found in [6].

Comments to Case Study 2

A strategy to identify an SDOF mechanical system with unknown nonlinearity using NIXO methods was presented in this section. A few comments on the results obtained are enumerated below.

1. In the first stage of the system identification process, NIXO methods using Eq. (26) as a model function were used. The outcomes from this stage showed that a cubic nonlinear stiffness was present in the mechanical system. Additionally, the nonlinear stiffness terms of powers lower than or equal to 6 were discovered to be less significant in the system's response.

2. In the second stage of the proposed strategy, NIXO methods used the model function presented in Eq. (27). The results from this stage showed that the cubic nonlinearity was also dominant over nonlinearities of higher powers.

3. NIFO methods did not work well when the mechanical system was excited with a swept cosine function. However, this type of forcing can be used as an input signal for the system identification based on the NIXO algorithms. Time did not allow exploring the use of broadband random forcing with NIFO, although the examples in the previous section showed that NIFO was more satisfactory in that case, typically similar to the NIXO method.

Conclusion and Future Work

This paper presented several new methods that can be successfully used in the estimation of the linear FRF as well as frequency-independent nonlinear parameters of a nonlinear system. The methods were first used in the system identification of a single degree of freedom system with the nonlinearity known à priori. Additionally, a black-box identification scheme utilizing the NIXO approaches was presented. Results were compared to those obtained using NIFO methods, which are popular approaches for nonlinear system identification.

Based on the outcomes presented in this work, it can be said that the NIXO algorithms show certain advantages over the NIFO approaches. First of all, the NIXO-based methods are not input-signal-sensitive. In the case studies used here, the NIFO algorithms required the mechanical system to be excited with a random forcing function. Furthermore, when considering black-box identification, NIXO methods turned out to be more effective than NIFO. The results returned by the former family of methods clearly showed that the cubic nonlinearity was dominant in the system response. The outcomes from the NIFO black-box identification did not show which nonlinear stiffness term was dominant in the system's response. Hence, they did not allow for making a confident decision on which of the nonlinear stiffness terms could be eliminated from the model function.

In a future work, both NIXO methods will be employed experimentally to identify the physical parameters describing the nonlinearity of a 3D printed beams for oscillations near their first vibration modes. The results will be then used to compute the NNM backbone curve and compared to the solution obtained by another estimation algorithm and data collected using the well-established testing approach.

Tab. 9: Additional nonlinear term degree: $r = 9$. Black (red) border around the bars indicates positive (negative) value.

	Linear FRF estimate	Nonlin. param. estimates	Nonlin. terms FFT ($x(t)$ – output signal)
$\mathbf{H}_1$-NIFO	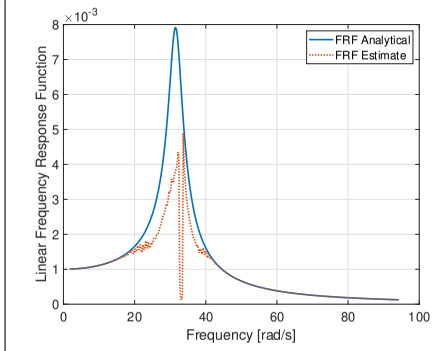	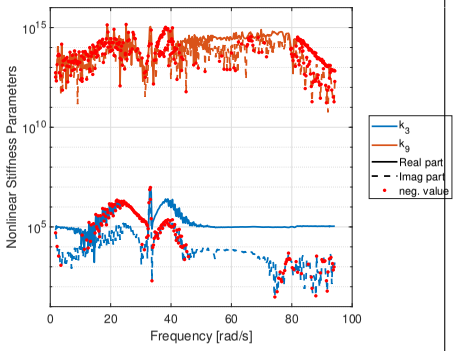	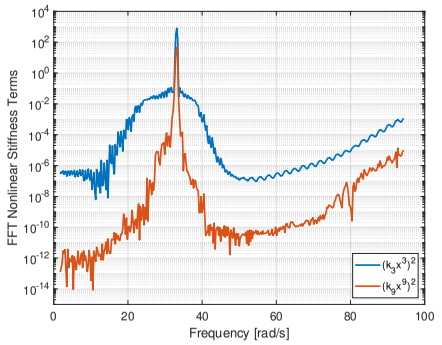
$\mathbf{H}_2$-NIFO	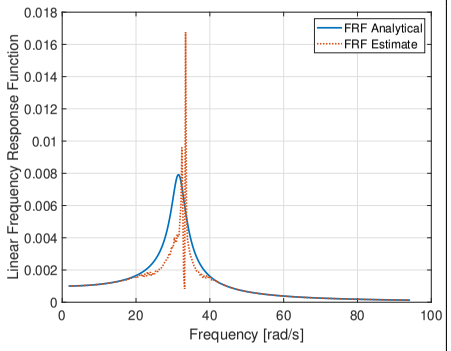	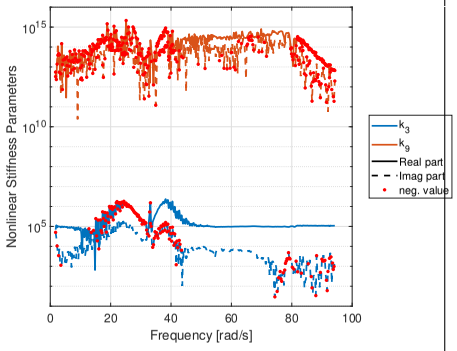	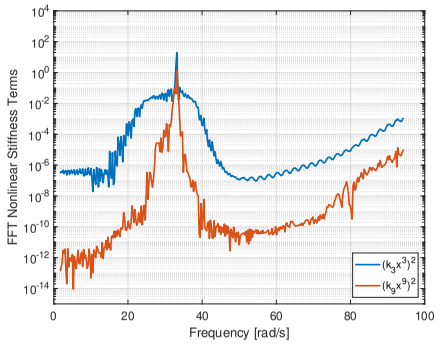
$\mathbf{H}_1$-NIXO	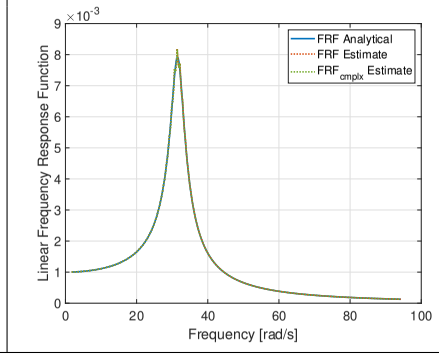	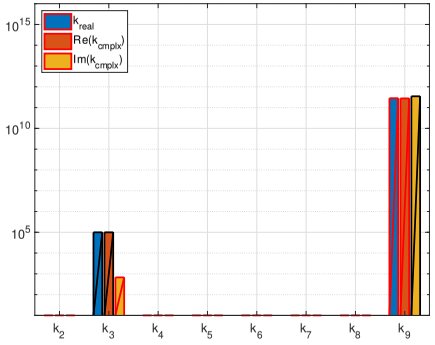	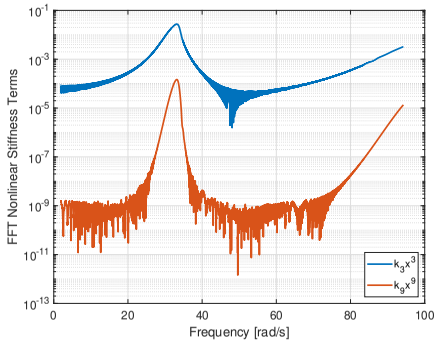

	Linear FRF estimate	Nonlin. param. estimates	Nonlin. terms FFT ($x(t)$ – output signal)
$\mathbf{H}_2$-NIXO	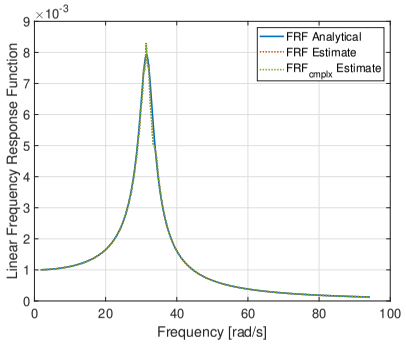	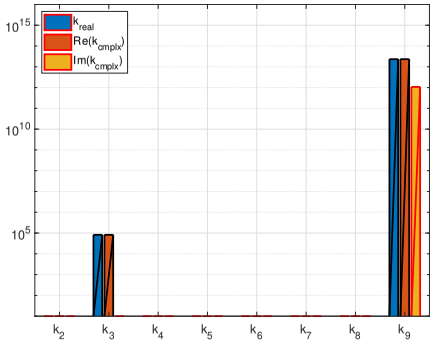	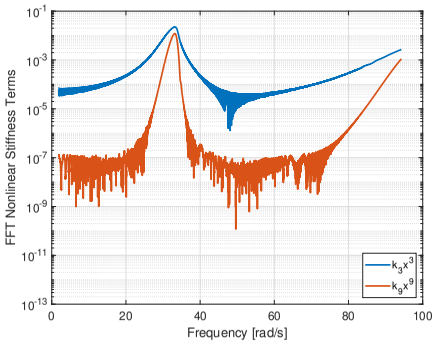
$\mathbf{H}_1$-NIXO WLDP	×	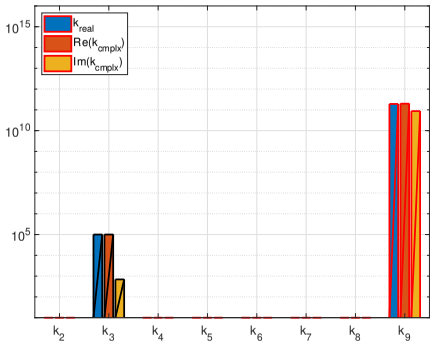	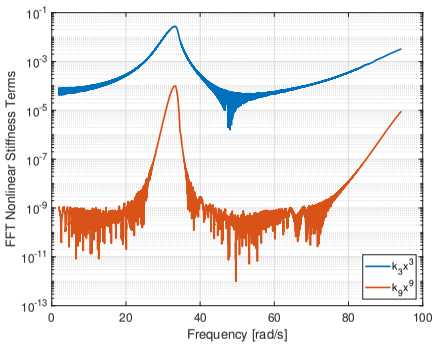
$\mathbf{H}_2$-NIXO WLDP	×	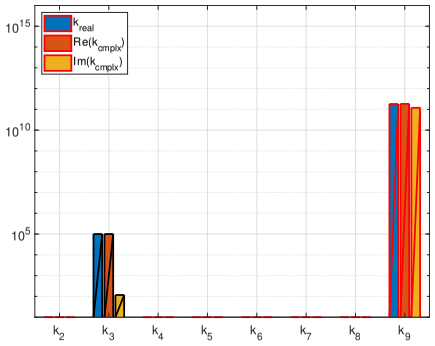	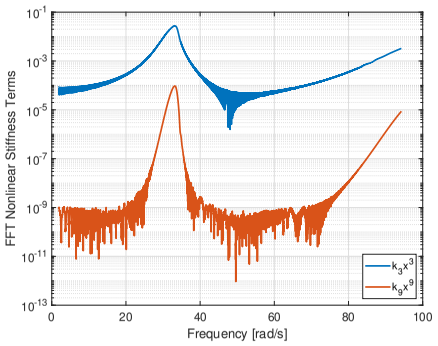

Acknowledgments This work was supported by the Air Force Office of Scientific Research, Award # FA9550-17-1-0009, under the Multi-Scale Structural Mechanics and Prognosis program managed by Dr. Jaimie Tiley. The authors would also like to thank Joseph Hollkamp from the Air Force Research Laboratory's Structural Sciences Center, for his insightful comments and suggesting several improvements to this work.

References

[1] Adams, D., and Allemang, R., 2000. "A frequency domain method for estimating the parameters of a non-linear structural dynamic model through feedback". *Mechanical Systems and Signal Processing,* **14**(4), pp. 637 – 656.

[2] Haroon, M., and Adams, D. E., 2009. "A modified H_2 algorithm for improved frequency response function and nonlinear parameter estimation". *Journal of Sound and Vibration,* **320**, 03, pp. 822–837.

[3] Kerschen, G., Lenaerts, V., and Golinval, J.-C., 2003. "Identification of a continuous structure with a geometrical non-linearity. part i: Conditioned reverse path method". *Journal of Sound and Vibration,* **262**(4), pp. 889 – 906.

[4] Noël, J., and Kerschen, G., 2017. "Nonlinear system identification in structural dynamics: 10 more years of progress". *Mechanical Systems and Signal Processing,* **83**, pp. 2 – 35.

[5] Kwarta, M., and Allen, M. S., 2019. "Derivation, Validation and Comparison of the NIFO and NIXO Algorithms for SDOF Systems". Available at "`https://sd.engr.wisc.edu/wp-content/uploads/sites/709/2019/10/NIXO_report_01_b.pdf`" (unpublished). Tech. rep.

[6] Kwarta, M., and Allen, M. S., 2019. "NIFO and NIXO Estimators for SDOF Systems: Impact of the Output Terms Choice on the Results". Available at "`https://sd.engr.wisc.edu/wp-content/uploads/sites/709/2019/10/NIXO_report_02.pdf`" (unpublished). Tech. rep.